

1 THE SWISS ATLAS OF PHYSICAL PROPERTIES OF ROCKS (SAPHYR)

Alba S. Zappone^{1-2*}, Rolf H. C. Bruijn

¹Institute of Process Engineering, ETH Zurich, Sonneggstrasse 3, 8092 Zurich, Switzerland

²Swiss Seismological Survey, Sonneggstrasse 5, 8092 Zurich, Switzerland

alba.zappone@sed.ethz.ch

ABSTRACT

Since 2007, a multi-year project runs under the umbrella of the Swiss Geophysical Commission, with the aim to digitize all existing data on physical properties of rocks and to link them using a geographical frame (GIS). The target is to make those data accessible to a wide public such as in industrial context, for land use planners and for academic studies. The physical properties considered are density and porosity, seismic, magnetic, thermal properties, permeability and electrical properties.

For the time being, data from literature has been collected extensively for seismic and magnetic properties and only partially for the other physical properties.

In this report we present the activity in the years 2010-2011, The main output has been two maps: a map of Switzerland combined with mean values of V_p , extrapolated to room conditions from the high pressure laboratory measurements (matrix or crack free properties), and a map describing the bulk density distribution on the Swiss territory.

1.1 METHODOLOGY

1.1.1 Data collection

SAPHYR, is comprised of 1) empirically acquired data published in scientific literature, theses and reports, and 2) new laboratory measurements performed on existing and newly obtained rock samples from Switzerland. In an effort to expand the SAPHYR database, previously overlooked literature data is added and new laboratory measurements are continuously undertaken. Here we present mainly the part related to bulk density and P-wave velocity. Other physical properties, such as S-wave velocity, seismic anisotropies, porosity and magnetic susceptibility are at present in the process of incorporation into the SAPHYR database.

Sample requirements

For the inclusion of data in the SAPHYR database five requirements have to be met: 1) the sample should be unequivocally identified (ID), 2) the coordinates of the sampling location should be available with a resolution of 100 m or 10 seconds, or should be construable from maps and sample descriptions within the aforementioned resolution, 3) a description of rock type should be present, 4) the rock sample should have originated from within Switzerland or from geological formations outcropping outside Switzerland but of relevance for the Swiss territory (approximately within 40 km distance from the political border).

For the time being the dbase refers only to samples that originate from outcrop; borehole and well-log data have not been included at the moment. In order to expand the dbase to depth the derivatives of the physical parameters with pressure and temperature are to be taken into account. At the moment those derivatives are systematically collected, but not elaborated in a way that would make them applicable to the scale of the geological formation or rock type

Utilized literature

At this point, the database consists of 529 viable literature samples, from 13 sources, published between 1976 and 2007 (Fountain 1976; Burke and Fountain 1990; Burlini and Fountain 1993; Sellami 1994; Barruol and Kern 1996; Zappone et al. 1996; Burlini et al. 1998; Wagner et al. 1999; Khazanehdari et al. 2000; Hölker 2001; Pera and Burlini 2001, Pros et al. 2003; Barberini et al. 2007).

Laboratory measurements

Besides literature data, included in the SAPHYR database are unpublished data from 264 samples that were measured for the first time in the Rock Deformation Laboratory at ETH Zurich. Cylindrical cores were drilled from collected rock samples in a direction either normal to foliation (z), parallel to lineation (x) or parallel to foliation and normal to lineation (y) (Figure 1b). 22 mm or 25.4 mm diameter cores were then trimmed or saw-cut to a length/diameter ratio of 2.0-2.5. Subsequently polish on fine-grained abrasive paper ensured parallelism between top and bottom surfaces and eliminated geometrical irregularities. Before they were tested, sample cores were dried in a 110 °C oven for at least 12 hours to remove possible fluids in the pore space.

Bulk density was determined as the ratio between dry mass (g) and bulk volume (cm³), using a digital mass balance (1 mg resolution) and digital caliper (10 µm resolution) measurements. When multiple cores from one rock sample or locality existed, the average bulk density was considered.

P-wave velocities (V_p), were determined using the pulse transmission technique (Birch 1960, 1961). Experiments were performed using either 1) a Paterson-type gas-medium testing machine (Paterson 1990), following technical modifications and experiment procedures described in e.g. Faccenda et al. (2007) and Almquist et al. (2010), or 2) an oil-medium hydrostatic pressure vessel modified for ultrasonic velocity testing (e.g. Wagner et al. 1999; Zappone et al. 2000). In regular pressure intervals, sample cores were exposed to increasing confining pressure to allow the derivation of the crack or porosity-free V_p extrapolated to room pressure (V_{p0}) (Figure 1a) (e.g. Birch 1961). For the Paterson apparatus, V_p was measured between 50 MPa and 400 MPa at 25 MPa intervals. The employed pressure range in the hydrostatic pressure vessel was 20 to 300 MPa, with 20 MPa intervals.

1.1.2 Sample matching

Matching evaluation

The conversion of sample point data to a physical properties map derived from a sample/lithology matching procedure that utilized the lithological information of the digital geotechnical map of Switzerland version 1/2000, issued by the Swiss Geotechnical Commission (SGTK)). Using an ESRI®-built ArcMap™ 9.3 environment, database samples were matched to a lithology type, on the basis of the rock type description and Swiss grid sample coordinates (datum CH1903 on 1841 Bessel ellipsoid) Sample matching was qualitatively evaluated by comparing the lithology type on the digital map and the rock type description of the sample. Sample matching was labeled as 'good', 'OK', 'poor' or 'bad', based primarily on proximity to a good lithological match. Effectively, these labels describe in a subjective and unquantified way, the decreasing usability of the sample for the construction of physical properties maps. The label 'good' is reserved for samples that plot, inside the same lithology type as the described rock type. The label 'OK' denotes either samples that plot within a few hundred meters of the same mapped lithology type as the described rock type (herein lie the assumptions that either the sample originated from an outcrop that is too small for appearance on the 1:500,000 digital geotechnical map), or samples that are geologically related in rock type description to the local lithology type, without exact matches within reasonable distance (for example a dolomite sample plotting in a limestone setting). The label

'poor' designates sample matches where only compositional correlation exists (e.g. a pelite sample matching with a metapelitic lithology type, or a marble sample plotting on a limestone lithology type). Finally, the label 'bad' is used for complete mismatches; that is, no geological correlation between sample rock type and regional lithology types. Mismatches probably originate from erroneous coordinates or coordinate systems, or incorrect rock type descriptions. Attempts were made to promote 'poor' and 'bad' matches to the status of 'OK' or 'good' by verifying the accuracy of sample coordinates (e.g. swapped xy coordinates) and correctness of the sample rock type description by thin section analysis. Data from remaining 'poor' and 'bad' matching samples were ignored in the construction of the physical properties maps.

Lithology groups (LG)

After the matching stage it became evident that the collected samples unevenly matched with lithology types on the map. In fact, emphasis is on the crystalline alpine lithologies, whereas some rare or unconsolidated lithology types are not matching at all. To reduce data gaps and improve map coverage, the original 69 specifically described lithology types were re-grouped into 28 general lithology groups (LG) (Table 1 and Figure 2). Additional advantage of the regrouping is the increase of data population for each lithology available. Disadvantageous, however, is the reduced resolution of the maps, as the number of unique values assigned to polygons of the digital geotechnical map lowered.

The lithology groups initially encompassed lithology types with geologically related rock type descriptions (Table 1). To recover map resolution, high-population ($n > 10$) lithology types were separated out from their lithology group and treated as stand-alone groups, provided the population size of the remaining lithology groups remained > 10 . This arbitrary value represents the minimum population size that is required to yield a geologically representative density or V_{p0} data distribution pattern.

The ultimate goal remains a classification of lithologies according to the digital geotechnical map, which allows maximum map resolution. As more samples are continuously included in the database, more lithology groups are anticipated to split into more specific lithology groups with unique physical properties.

Data presentation

Statistical information for each lithology group is presented in table, histogram and map format. Statistical data included in tables is comprised of 1) population size (n), 2) minimum, median and maximum values, 3) mean and standard deviation (σ) calculation, and 4) assuming a Gaussian distribution, one standard deviation interval (σ -interval) calculations. The σ -interval represents the 68.3 area % of the Gaussian distribution model, around the mean value (i.e. there is a 68.3 % probability that the value for density or V_{p0} of a sample is within the σ -interval). Supplementary information includes a qualitative and subjective description of the binned data distribution (i.e. low n , no data, normal, scattered, or negative/positive skew), and the binned range of the data (Δ = the range between the minimum and maximum interval with data). For water (LG 25) and ice (LG 26) no statistical data is available, as only the generally known values for density and P-wave velocity are considered. Histograms with 0.1 g cm^{-3} or 0.5 km s^{-1} discrete intervals (bins) for density and V_{p0} , respectively, visualize the data distribution for each lithology group. For the visualization in map format of bulk density and V_{p0} distribution across Switzerland, mean values are utilized. These maps are constructed by coupling mean values for each lithology group to polygons provided by the digital geotechnical map. Additional maps show the distribution of the calculated bulk density and V_{p0} standard deviation. These complementary maps visualize in essence, the distribution of the quality of the mean values and thus act as quality control maps. Important however, quality here does not necessarily reflect a statistical or geological origin for the standard deviation value. It rather reflects how well the mean value represents the variation in the data

1.2 RESULTS

Due to easy access and excellent outcrop conditions, not surprisingly, the vast majority of samples originate from the Alps in southern Switzerland and northern Italy (Figure 2). In comparison with the Alps, sampling in the Jura and Swiss central plateau (Mittelland) is underdeveloped. However, some lithology groups that surface in the latter two geographical regions also crop out in the Alps (Figure. 2).

In total, 793 samples with density and/or Vp0 data have been judged viable for inclusion in the SAPHYR database, out of which 49.2 % have a 'good' lithology type or group match, 37.1 % an 'OK' match, and 11.2 % and 2.5 %, respectively a 'poor' and 'bad' match. Within the three geographical regions of Switzerland, and in the bordering countries, nearly all matching evaluation grades can be found (Figure. 2). Only in the Jura, bad matches could be avoided.

1.2.1 Bulk density

Lithology groups statistics

A total of 602 bulk density measurements have been linked to one of 22 lithology groups. Therefore, sample-matching left 6 lithology groups without data (Table 2). For 10 lithology groups with population size $n > 10$, bulk density data display a normal distribution with standard deviation values below 0.14 g cm⁻³ (Figure. 3 and Table 2). The distribution for 4 lithology groups cannot be adequately described due to low sample population size ($n < 10$). Mean values among lithology groups range between 2.31 g cm⁻³ for unconsolidated debris (LG 28) and 3.23 g cm⁻³ for ultramafics (LG 21). All samples combined show a normal density data distribution between 1.9 and 3.5 g cm⁻³, with a standard deviation of 0.22 g cm⁻³, and mean at 2.78 g cm⁻³. Separated into sedimentary rocks (Figure. 3a-b), upper crustal rocks (Figure. 3c-d) and lower crustal / upper mantle rocks (Figure. 3e), with increasing typical burial depth, distribution of the density data displays the expected shift to denser rocks and reduced scatter among lithology groups,

Mean bulk density map

The mean bulk density values for 22 lithology groups are visualized on a map of Switzerland (Figure 4a). This map shows that density of rock at the surface is variable throughout Switzerland. Most apparent is the density contrast between crystalline rocks of the Alps and to a lesser extent the Jura, and the recent alpine valley infill and Molasse basin cover of the Mittelland (Figure 4a).

Bulk density standard deviation map

The representativeness of the mean density value for each lithology group, by not considering the natural variation and complexity of geological processes that affect density, is effectively expressed by the bulk density standard deviation. With increasing standard deviation values, the mean value for a lithology group becomes less characteristic (i.e. quality decreases). The map of the bulk density standard deviation effectively shows the quality of the mean bulk density values in Switzerland (Figure 4b).

In comparison with the mean bulk density map (Figure 4a), the standard deviation map (Figure 4b) conceals the presence of three major geographic features in Switzerland. The high standard deviation values of calc-shales/slates (LG 4) and unconsolidated debris (LG 28) visually contrast sharply with the other 22 lithology groups in the Jura, Mittelland and Alps (Figure 4b). Nevertheless, in the Jura, colours representing low values for the standard deviation dominate, whereas in the Alps, low, intermediate and high standard deviation values are all showing in more or less equal frequency.

1.2.2 P-wave velocity extrapolated to room pressure (V_{p0})

Lithology groups statistics

A total of 447 Vp0 measurements have been linked to one of 22 lithology groups, leaving 6 lithology groups without data (Table 3). For 13 lithology groups with population size $n > 10$, Vp0 data display a normal distribution with standard deviation between 0.22 and 0.56 km s⁻¹. The distribution for 6 lithology groups cannot be described with confidence due to low sample population size ($n < 10$). The highest Vp0 standard deviation was found for quartzites (LG 19), with a standard deviation of 0.85 km s⁻¹. For this lithology group and five others the binned range was highest with $\Delta = 3.0$ km s⁻¹, although absolute boundaries vary (Table 3). Mean values among lithology groups range between 4.13 km s⁻¹ for porous sandstones (LG 2) and 7.66 g cm⁻³ for ultramafics (LG 21). All samples combined show a normal Vp0 distribution between 2.5 and 9.0 km s⁻¹, with a standard deviation of 0.74 km s⁻¹, and mean at 6.16 km s⁻¹. Separated into sedimentary rocks (Figure 5a-b), upper crustal rocks (Figure 5c-d) and lower crustal / upper mantle rocks (Figure 5e), with increasing deeper origin, distribution of the Vp0 data, except

serpentinites (LG 20), displays the expected shift to faster P-waves, with exception for serpentinites (LG 20). In addition, Vp0 in carbonates is slightly faster than in siliceous sediments (Figure 5a-b). Among upper crustal rocks, mica-rich lithologies have a lower Vp0 than mica-poor lithologies (Figure 5c-d). In fact, also for most sedimentary rocks, Vp0 is faster than for upper crustal mica-rich rocks (Figure 5a-c).

Mean Vp0 map

The mean of Vp0 for 22 lithology groups are visualized on a map of Switzerland (Figure 6a). Three geographical areas can be identified from the mean Vp0 map (Figure 6a): 1) in the northwest of Switzerland relatively high velocities represented in orange dominate, 2) in the Mittelland lower Vp0 values (down to 4.1 km s⁻¹) dominate, and 3) throughout the south, not considering lakes and glaciers, velocity contrasts among lithology groups (orange tints dominate) give rise to a complex color pattern. The subdivision of P-wave velocity domains corresponds exactly to the appearance of crystalline rocks at the surface (Figure 2), with high velocities in the Jura and Alps, and contrastingly low velocities in soft-sediments of the Mittelland. Similarly, soft sediments in alpine valleys are recognized by their low mean Vp0 (Figure 6a),

Mean Vp0 standard deviation map

Similar to the mean bulk density, the representativeness of the mean Vp0 value of the generalized lithology groups is effectively expressed by the Vp0 standard deviation. Larger standard deviation values indicate lesser representativeness (i.e. quality decreases) of the mean value. The map of the Vp0 standard deviation shows the quality of mean Vp0 values in Switzerland (Figure 6b).

Like for the mean Vp0 map (Figure 6a), the standard deviation map (Figure 6b) clearly shows the three major geographical features in Switzerland. In the Jura, low standard deviation values dominate, whereas in the Mittelland most outcropping lithology groups have a higher Vp0 standard deviation. In the Alps, standard deviation varies between low and high values, although the former dominate the overall appearance. There, most high standard deviation values appear in alpine valleys and rarely represent crystalline lithology groups. In fact, standard deviation values for crystalline rocks are lower than for sediments. The lowest standard deviation is found for crystalline lithology groups in central southern Switzerland (Figure 6b).

1.3 FIGURES, AND TABLES

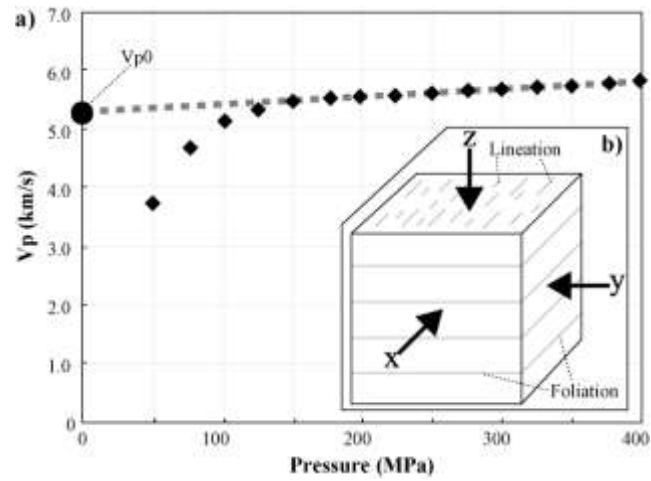


Figure 1. Typical curve for a P-wave velocity test in the Paterson apparatus, with increasing confining pressure. V_{p0} is derived by linear extrapolation of the high-pressure V_p behavior back to room pressure. In the insert the definition of sample drilling directions is shown.

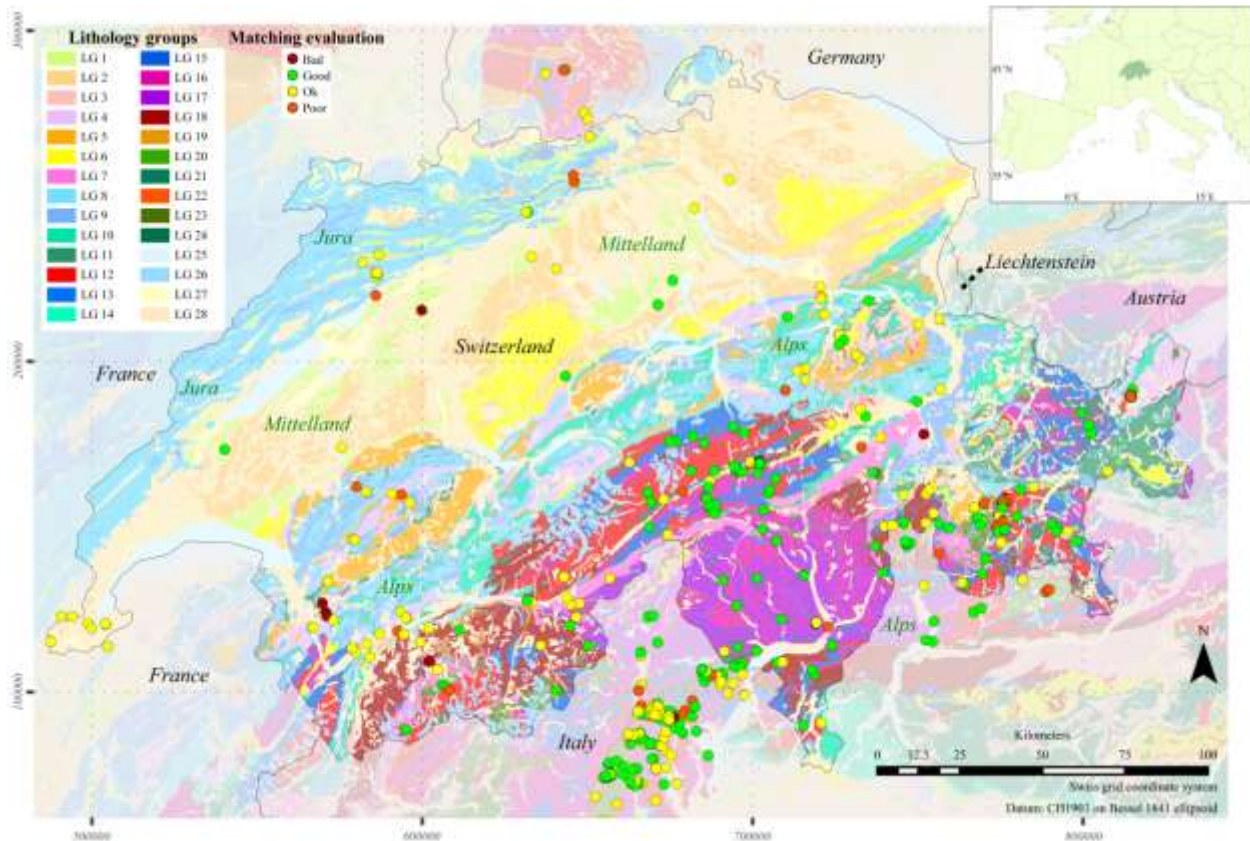


Figure 2. Modified SGK geotechnical map of Switzerland showing 28 lithology groups and the SAPHYR database samples with V_{p0} and/or bulk density data, colour coded according to the evaluation of the match with the original lithology type on the map. Classification and description of lithology groups is presented in Table 1.

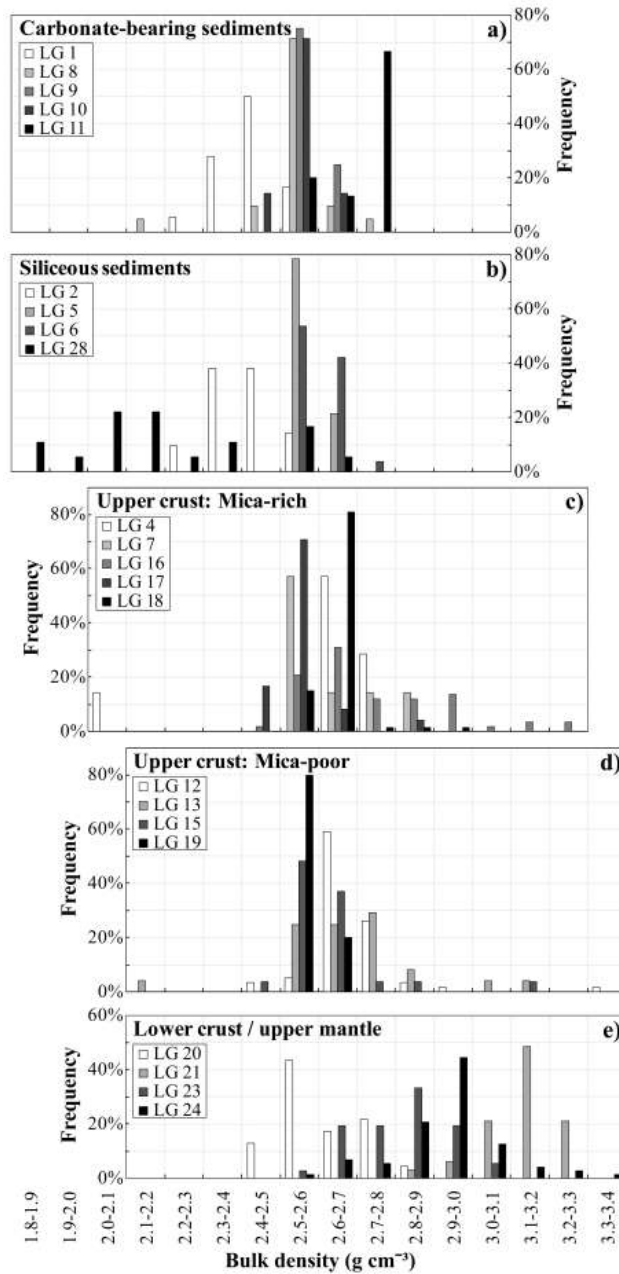


Figure 3 Bulk density histograms displaying frequency against binned bulk density values for 22 lithology groups (LG) divided into five generic groups: lithology groups that consist of a) carbonate-bearing sediments, b) siliceous sediments, c) upper crustal rocks in which mica minerals dominate, d) upper crustal rocks in which mica minerals are of secondary importance in terms of composition, and e) typical lower crustal or upper mantle rocks.

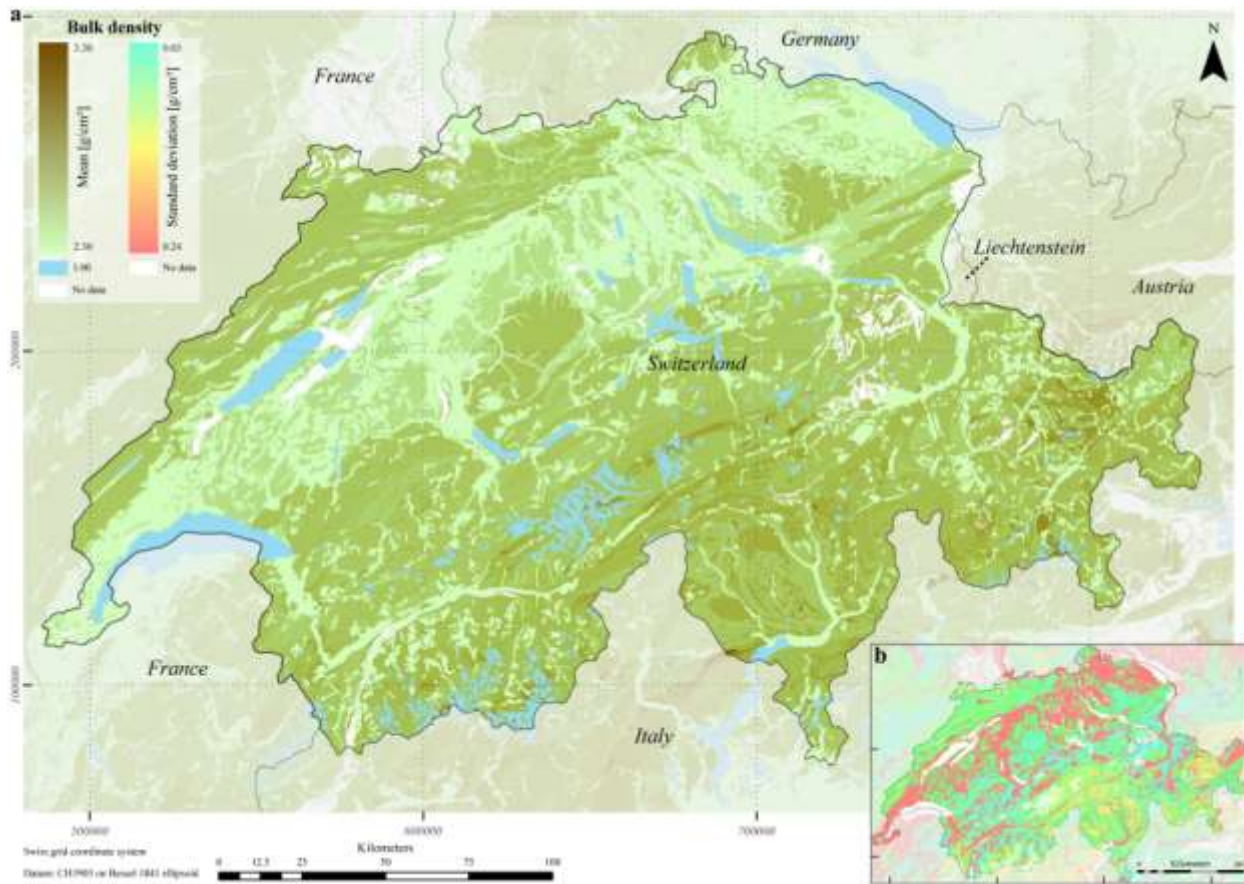


Figure 4 Map showing the distribution of mean bulk density data in the SAPHYR database. Using a colour ramp ranging from light green (2.30 g cm^{-3}) to brown (3.30 g cm^{-3}), mean density is shown as a function of colour. The assumed lower density-value for water and ice, representing lakes and glaciers, is displayed in supplementary light blue tints. The insert shows the distribution of standard deviation data for bulk density data of lithology groups in Switzerland. The distribution is visualised with a partial rainbow colour ramp that ranges from turquoise-greenish colours ($\sigma = 0.03\text{-}0.10 \text{ g cm}^{-3}$) to light orange-reddish colours ($0.15\text{-}0.24 \text{ g cm}^{-3}$). Lithology groups with no data (i.e. assumed values or absence of samples) are shown in white.

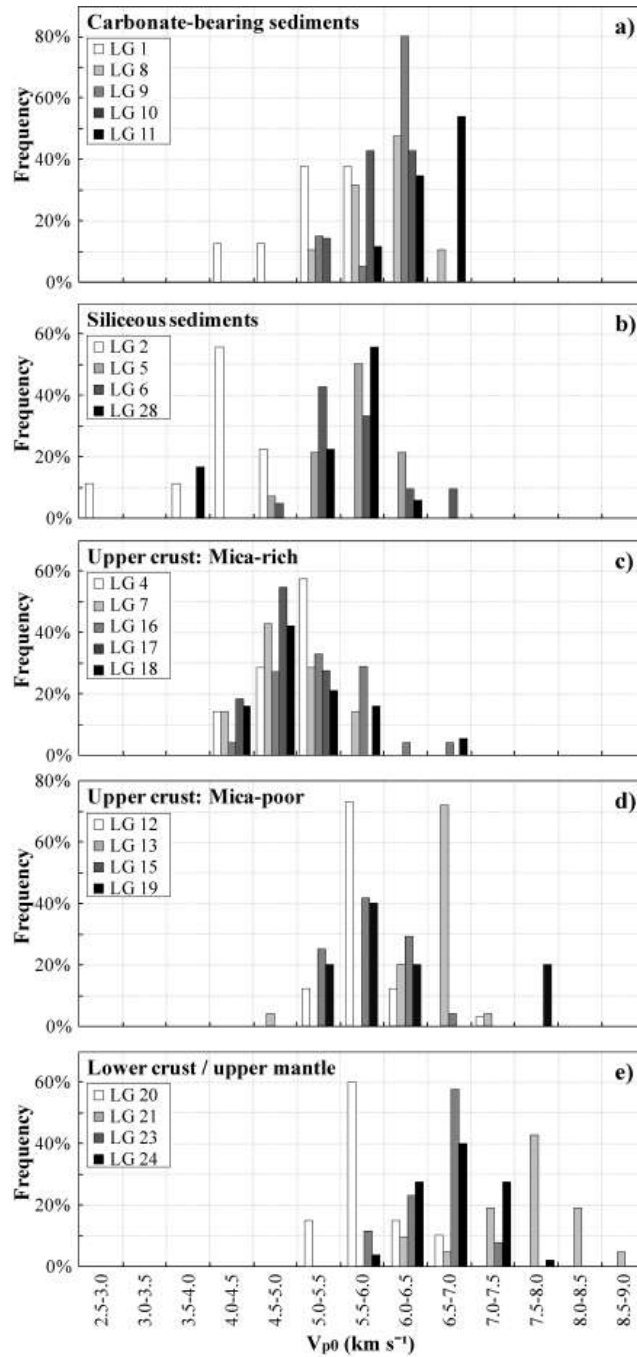


Figure 5 V_{p0} histograms displaying frequency against binned V_{p0} values for 22 lithology groups (LG) divided into five convenient generic groups: lithology groups that consist of a) carbonate-bearing sediments, b) siliceous sediments, c) upper crustal rocks in which mica minerals dominate, d) upper crustal rocks in which mica minerals are of secondary importance in terms of composition, and e) typical lower crustal or upper mantle rocks.

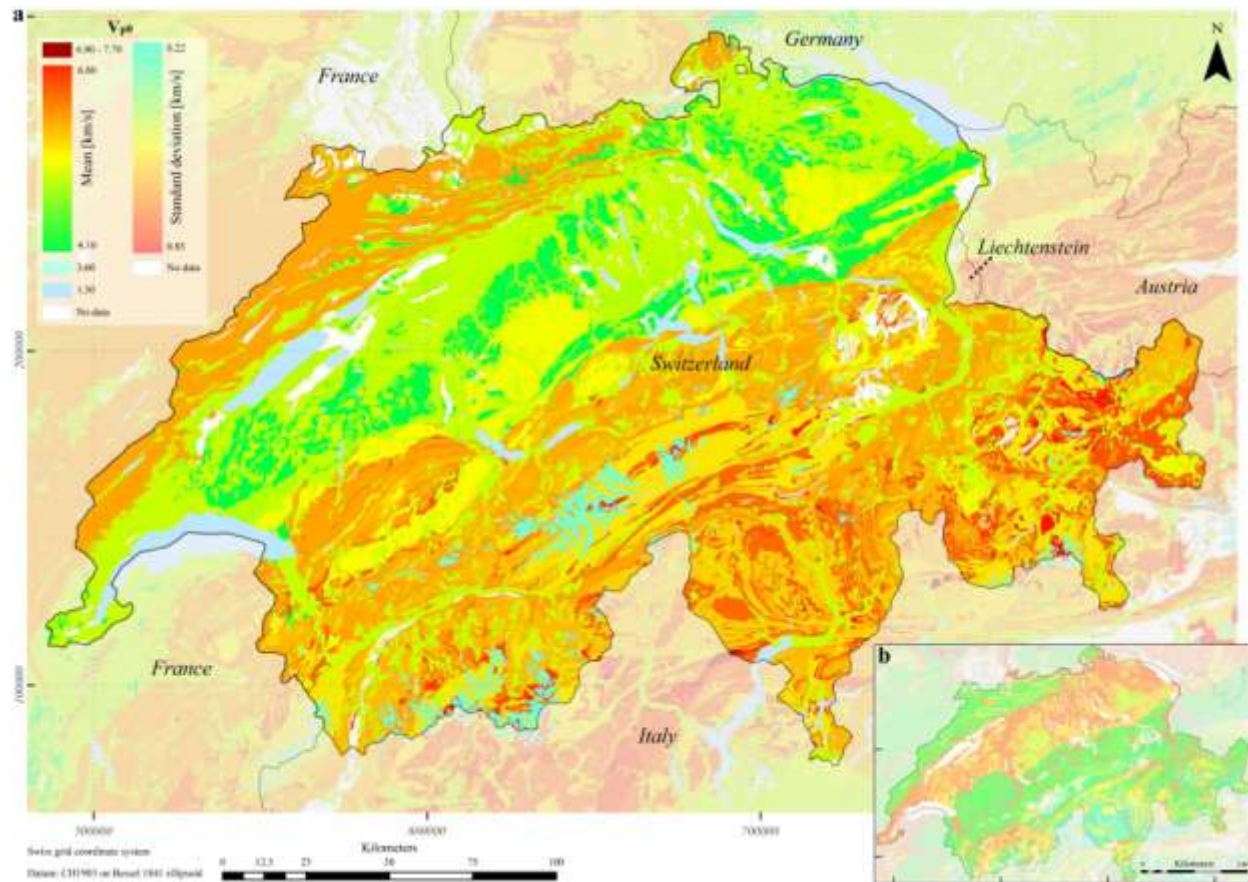


Figure 6 a) Distribution of mean V_{p0} data in the SAPHYR database. Using a partial rainbow colour ramp ranging from green (4.10 km s^{-1}) to red (6.80 km s^{-1}), mean V_{p0} is shown as a function of colour. The assumed velocity-values for water and ice, and the calculated mean V_{p0} for ultramafics (LG 21) are displayed in supplementary light bluish colours and dark red, respectively. The latter lithology group was excluded from the partial colour ramp range to enhance colour contrast among the other lithology groups. b) Miniature map showing the distribution of standard deviation data for V_{p0} data of lithology groups in Switzerland. The distribution is visualized with a partial rainbow colour ramp that ranges from turquoise-greenish colours ($\sigma = 0.22\text{-}0.40 \text{ km s}^{-1}$) to light orange-reddish colours ($0.60\text{-}0.85 \text{ km s}^{-1}$). Lithology groups with no data (i.e. assumed values or absence of samples) are shown in white.

Table 1. Subdivision of lithology types from the SGK geotechnical map in lithology groups.

GeoTech ID ¹	Lithology type description	Lithology group	Field count ²
10	Marl with badly consolidated sand, pebbles or debris layers		
12	Marl with layers of shell-rich sandstone to breccia		
13	Marly clay and shale with banks of carbonate or sandstone	LG 1	1146
15	marl with dense sandstone layers	Marls	
17	Marl with layers of dense shell-rich sandy breccia		
11	Predominantly calcareous, porous sandstone with layers of marl	LG 2	
16	Sandstone with layers of marl	Porous sandstones	880
21	Sandstone and marl layers with unconsolidated conglomerate		
14	Ferrous clay		
18	Slate with layers of limestone/gypsum/sandstone/rauhwacke	LG 3	352
30	Slate to phyllite with sandstone or breccia/conglomerate layers	Mudstones/shales/slates	
55	Quartz-phyllite		
31	Marly slate to calc-phyllite with layers of sandstone	LG 4	590
33	Marly slate to calc-phyllite with layers of tuff sandstone	Calc-shales/slates	
19	Quartz-sandstone to sandy slate		
32	Dense sandstone with layers of marly slate and calc-phyllite	LG 5	432
45	Glauconite quartz sandstone with echinoderm fragments	Compact sandstones	
20	Conglomerate with sandstone and marl layers		
22	Conglomerate/breccia with arkose and sandstone		
23	Breccia and conglomerate	LG 6	437
46	Calcareous breccia or conglomerate	Conglomerates/ breccias	
64	Sericite-rich conglomerate and breccia		
35	Calc-phyllite to calc-micaschist		
36	Calc-phyllite to calc-micaschist with layers of marble	LG 7	332
37	Calc-phyllite to calc-micaschist with layers of green rocks	Calc-slate/schists	
40	Limestone, frequently with marly layers	LG 8 Marly limestones	2148
38	Limestone with layers of dolomite		
41	Limestone, often a bit marly	LG 9	1476
42	Limestone with clear layers of (calc) marl and marly slate	Mixed carbonates	
43	Calcareous gravel	LG 10	528
44	Coarse limestone with layers of marly slates	Siliceous limestones	
47	Dolomite, partly with limestone layers		
48	Dolomite and rauhwacke	LG 11	1472
49	Dolomite with evaporite layers	Dolomites	

50	Granite with transitions into quartz diorite and syenite		
51	Granite with sericite, epidote and chlorite		
52	Quartz porphyry	LG 12	687
53	Syenite	Granitoids	
54	Porphyrite and porphyrite tuff		
56	Limestone and marble	LG 13	323
57	Dolomitic marble	Marbles	
58	Radiolarite	LG 14 Radiolarites	42
60	Feldspar-rich gneisses	LG 15	686
61	Feldspar gneiss with sericite/chlorite/epidote overprint	Feldspar gneisses	
62	Biotite/muscovite gneiss and micaschist	LG 16 ????????	694
59	Mica/biotite/feldspar gneiss with mixed structures		
65	Mica/biotite/feldspar gneiss with homogeneous structures	LG 17	158
66	Platy mica/biotite/feldspar gneiss	Mica feldspar gneisses	
63	Sericite/chlorite gneiss/schist		
67	Mica/biotite gneiss with bright, often green phengite	LG 18	442
68	Mica/biotite gneiss, with chlorite, calc-silicates or quartzite	Mica schist/gneisses	
637	Quartz/sericite/chlorite gneiss/schist with amphibolite layers		
69	Quartzite	LG 19 Quartzites	112
70	Serpentinite	LG 20 Serpentinites	151
71	Peridotite and dunite	LG 21 Ultramafics	57
75	Volcanics and pyroclastics	LG 22 Volcanics	21
81	Greenschist with transitions to basic extrusives and eclogite	LG 23 Metagabbro	322
80	Amphibolite with transitions to diorite and hornblende gneiss		
83	Diorite and gabbro	LG 24	454
84	Mixture zone between amphibolite and gneiss	Mafics	
90	Surface water and lakes	LG 25 Water	590
99	Glacier	LG 26 Ice	523
111	Silt to silty sands, often clayey, mostly calcareous	LG 27	573
112	Clayey silt to clay with sandy layers	Fine-grained deposits	
110	Silt to sand bodies, with gravel, rocks and debris blocks		
120	Gravel and sand		
130	Gravel and sand, partially with clay or silt layers	LG 28	7438
131	Sand, gravel, pebbles, stones and debris blocks	Unconsolidated debris	
132	Debris blocks and scree material		

¹ Taken from the digital geotechnical map of Switzerland Version 1/2000

² Number of polygons in the digital geotechnical map of Switzerland Version 1/2000

Table 2. Bulk density data for the 28 lithology groups currently considered for the density map (Figure 2).

Lithology group	Description	Population n	Distribution	Mean (g cm ⁻³)	Median (g cm ⁻³)	Minimum (g cm ⁻³)	Maximum (g cm ⁻³)	S
LG 1	Marls	18	Normal	2.52	2.52	2.31	2.67	0
LG 2	Porous sandstones	21	Normal	2.51	2.51	2.32	2.62	0
LG 3	Mudstones/shales/slates	0	No data	-	-	-	-	-
LG 4	Calc-shales/slates	7	Low n	2.61	2.70	2.10	2.71	0
LG 5	Compact sandstones	14	Positive skew	2.68	2.67	2.64	2.73	0
LG 6	Conglomerates/breccias	26	Positive skew	2.71	2.70	2.61	2.81	0
LG 7	Calc-slates/schists	7	Low n	2.77	2.70	2.70	2.97	0
LG 8	Marly limestone	21	Normal	2.67	2.69	2.30	2.81	0
LG 9	Mixed carbonates	12	Positive skew	2.70	2.69	2.67	2.75	0
LG 10	Siliceous limestones	7	Low n	2.68	2.69	2.58	2.71	0
LG 11	Dolomites	15	Scatter	2.79	2.83	2.67	2.86	0
LG 12	Granitoids	61	Normal	2.69	2.68	2.46	3.33	0
LG 13	Marbles	24	Scatter	2.79	2.78	2.30	3.22	0
LG 14	Radiolarites	0	No data	-	-	-	-	-
LG 15	Feldspar gneisses	27	Normal	2.72	2.68	2.59	3.22	0
LG 16	Biotite micaschist/gneisses	58	Scatter	2.85	2.80	2.60	3.33	0
LG 17	Mica feldspar gneisses	24	Normal	2.65	2.63	2.55	2.96	0
LG 18	Mica schist/gneisses	73	Normal	2.74	2.74	2.63	3.01	0
LG 19	Quartzites	5	Low n	2.67	2.66	2.64	2.73	0
LG 20	Serpentinities	23	Scatter	2.72	2.70	2.58	2.92	0
LG 21	Ultramafics	33	Normal	3.23	3.24	2.96	3.35	0
LG 22	Volcanics	0	No data	-	-	-	-	-
LG 23	Metagabbro	36	Normal	2.92	2.92	2.67	3.13	0
LG 24	Mafics	72	Normal	3.03	3.05	2.68	3.43	0
LG 25	Water	0	-	1	1	1	1	1
LG 26	Ice	0	-	1	1	1	1	1
LG 27	Fine-grained deposits	0	No data	-	-	-	-	-
LG 28	Unconsolidated debris	18	Scatter	2.31	2.28	1.97	2.71	0
Total	All viable density measurements	602	Normal	2.78	2.73	1.97	3.43	0

Table 3. V_{p0} data for the 28 lithology groups currently considered for the P-wave map (Figure 3).

Lithology group	Description	Population n	Distribution	Mean (km s ⁻¹)	Median (km s ⁻¹)	Minimum (km s ⁻¹)	Maximum (km s ⁻¹)
LG 1	Marls	8	Low n	5.24	5.33	4.14	5.99
LG 2	Porous sandstones	9	Low n	4.13	4.23	2.66	4.72
LG 3	Mudstones/shales/slates	0	No data	-	-	-	-
LG 4	Calc-shales/slates	7	Low n	5.96	6.07	5.38	6.37
LG 5	Compact sandstones	14	Normal	5.66	5.65	4.96	6.13
LG 6	Conglomerates/breccias	21	Normal	5.60	5.54	5.00	6.75
LG 7	Calc-slates/schists	7	Low n	6.02	5.98	5.32	6.77
LG 8	Marly limestone	19	Normal	6.06	6.06	5.38	6.56
LG 9	Mixed carbonates	20	Negative skew	6.06	6.11	5.32	6.48
LG 10	Siliceous limestones	7	Low n	5.95	5.89	5.48	6.44
LG 11	Dolomites	26	Negative skew	6.49	6.50	5.93	6.93
LG 12	Granitoids	33	Normal	5.77	5.70	5.04	7.07
LG 13	Marbles	25	Normal	6.53	6.61	4.67	7.01
LG 14	Radiolarites	0	No data	-	-	-	-
LG 15	Feldspar gneisses	24	Normal	5.76	5.67	5.10	6.71
LG 16	Biotite micaschist/gneisses	52	Normal	6.33	6.35	5.37	7.96
LG 17	Mica feldspar gneisses	11	Normal	5.85	5.91	5.39	6.07
LG 18	Mica schist/gneisses	19	Normal	5.99	5.89	5.32	7.61
LG 19	Quartzites	5	Low n	6.17	5.83	5.48	7.62
LG 20	Serpentinites	20	Normal	5.86	5.85	5.21	6.84
LG 21	Ultramafics	21	Normal	7.66	7.83	6.27	8.53
LG 22	Volcanics	0	No data	-	-	-	-
LG 23	Metagabbro	26	Normal	6.57	6.63	5.57	7.29
LG 24	Mafics	55	Normal	6.74	6.69	5.89	7.55
LG 25	Water	0	Fixed	1.50	1.50	1.50	1.50
LG 26	Ice	0	Fixed	3.60	3.60	3.60	3.60
LG 27	Fine-grained deposits	0	No data	-	-	-	-
LG 28	Unconsolidated debris	18	Scatter	5.36	5.64	3.70	6.15
Total	All viable V_{p0} measurements	447	Normal	6.16	6.11	2.66	8.53

1.4 REFERENCES

- Almqvist, B.S.G., Burlini, L., Mainprice, D., Hirt, A.M. (2010). Elastic properties of anisotropic synthetic calcite-muscovite aggregates. *Journal of Geophysical Research*, 115.
- Barberini, V., Burlini, L., Zappone, A. (2007). Elastic properties, fabric and seismic anisotropy of amphibolites and their contribution to the lower crust reflectivity. *Tectonophysics*, 445, 227-244.
- Barruol, G., & Kern, H. (1996). Seismic anisotropy and shear-wave splitting in lower-crustal and upper-mantle rocks from the Ivrea Zone—experimental and calculated data. *Physics of the Earth and Planetary Interiors*, 95, 175-194.
- Birch, F. (1960). The velocity of compressional waves in rocks to 10 kilobars, part 1. *Journal of Geophysical Research*, 65, 1083-1102.
- Birch, F. (1961). The velocity of compressional waves in rocks to 10 kilobars, part 2. *Journal of Geophysical Research*, 66, 2199-2224.
- Burke, M.M., & Fountain, D.M. (1990). Seismic properties of rocks from an exposure of extended continental crust—new laboratory measurements from the Ivrea Zone. *Tectonophysics*, 182, 119-146.
- Burlini, L., & Fountain, D.M. (1993). Seismic anisotropy of metapelites from the Ivrea-Verbanò zone and Serie dei Laghi (northern Italy). *Physics of the Earth and Planetary Interiors*, 78, 301-317.
- Burlini, L., Marquer, D., Challandes, N., Mazzola, S., Zangarini, N. (1998). Seismic properties of highly strained marbles from the Splügenpass, central Alps. *Journal of Structural Geology*, 20, 277-292.
- Carmichael, R. (1989) Practical handbook of physical properties of rocks and minerals, CRC-Press, pp 741.
- Faccenda, M., Bressan, G., Burlini, L. (2007). Seismic properties of the upper crust in the central Friuli area (northeastern Italy) based on petrophysical data. *Tectonophysics*, 445, 210-226.
- Fountain, D.M. (1976). The Ivrea—Verbanò and Strona-Ceneri Zones, Northern Italy: A cross-section of the continental crust—New evidence from seismic velocities of rock samples. *Tectonophysics*, 33, 145-165.
- Hölker, A.B. (2001). Seismic structure and response of ocean-continent transition zones in magma-poor rifted continental. *Ph.D dissertation*, ETH Zurich, Zurich, Switzerland, 132 pp.
- Ji, S., Wang, Q., Xia, B. (2004) Handbook of Seismic Properties of Minerals, Rocks and Ores, Polytechnique International Press, pp630
- Kern, H. (1990). Laboratory seismic measurements: an aid in the interpretation of seismic field data. *Terra Nova*, 2, 617-628.
- Khazanehdari, J., Rutter, E.H., Brodie, K.H. (2000). High-pressure-high-temperature seismic velocity structure of the midcrustal and lower crustal rocks of the Ivrea-Verbanò zone and Serie dei Laghi, NW Italy. *Journal of Geophysical Research*, 105, 13843-13858.
- Paterson, M.S. (1990). Rock deformation experimentation, In A.G. Duba (Ed.), *The Brittle-Ductile Transition in Rocks. The Heard Volume* (pp. 187-194). Washington D.C.: AGU
- Pera, E., & Burlini, L. (2001). Elastic properties of selected Italian marbles. In R. Přikryl & H.A. Viles (Eds.), *Understanding and Managing Stone Decay* (pp. 261-272). Prague: Karolinum Press.
- Pros, Z., Lokajčiček, T., Přikryl, R., Klíma, K. (2003). Direct measurement of 3D elastic anisotropy on rocks from the Ivrea zone (Southern Alps, NW Italy). *Tectonophysics*, 370, 31-47.
- Sellami, S. (1994). Propriétés physiques de roches des Alpes suisses et leur utilisation à l'analyse de la réflectivité de la croûte alpine. *Ph.D. dissertation*, University of Geneva, Geneva, Switzerland, 175 pp.

Swiss Geotechnical Commission (SGTK) geotechnical map of Switzerland version 1/2000, ?????see how to quote it

Wagner, J.-J., Gong, G., Sartori, M., Jordi, S., Rosset, P. (1999). *A catalogue of physical properties of rocks from the Swiss Alps and nearby areas (No. 33)* (81 pp.). Zurich: Swiss Geophysical Commission.

Wepfer, W., & Christensen, N. (1991). A seismic velocity-confining pressure relation, with applications. *International Journal of Rock Mechanics and Mining Sciences & Geomechanics Abstracts*, 28, 451-456.

Zappone, A., Fernández, M., García-Dueñas, V., Burlini, L. (2000). Laboratory measurements of seismic P-wave velocities on rocks from the Betic chain (southern Iberian Peninsula). *Tectonophysics*, 317, 259-272.

Zappone, A.S., Sciesa, E., Rutter, E.H. (1996). Caratterizzazione sperimentale dei parametri elastici dello gneiss granitico di Leventina (canton Ticino, Svizzera). *Geologia Insubrica*, 1, 7-16.